

LETTER

Strong light confinement and gradient force in parallel infinite-width monolayer graphene pairs

To cite this article: Chunyu Lu et al 2019 Appl. Phys. Express 12 075007

View the <u>article online</u> for updates and enhancements.

LETTER

Strong light confinement and gradient force in parallel infinite-width monolayer graphene pairs



Chunyu Lu^{1,2}, Zheng-Da Hu¹, Jin Cui², Jicheng Wang^{1*}, and Liang Pan²

Received May 5, 2019; revised May 27, 2019; accepted June 3, 2019; published online June 17, 2019

We study high light confinement, field enhancement, and strong gradient force between graphene nanoribbons. Influence of the wavelength of incident light on the gradient force, which is rare in previous studies, is presented. Results of light field confinement are achieved, which are much better than those in the slot waveguides based on artificial hyperbolic metamaterials. The propagation length and enhancement ratio can be up to 79.5 μ m and 16, respectively. It is worth mentioning that the light confinement ratio can reach an astonishing 97%. Finally, we analyze the gradient force of different intensity in terms of the electric field. © 2019 The Japan Society of Applied Physics

he potential for optical force to move micron-sized particles was found by A. Ashkin when he performed experiments on the interaction of microscopic particles with focused light in 1969. On account of the original observation, he put forward a scheme to trapping particles by two focused lasers that propagated in the contrary directions. Optical forces have drawn much attention in recent years. Optical and mechanical systems with ultra small-mass and ultra high-mechanical-frequency as well as strong optical gradient force are especially desirable. 2-5) The optical gradient force has been utilized for activating optical waveguides. 6) The gradient force will result in nanometers or micrometers of mechanical displacements of two adjacent waveguides. Optical gradient forces are related to a lot of astonishing phenomena, like photoelectric mechanical sensing,⁷⁾ synchronisation of nanomechanical oscillators,⁸⁾ optical nonreciprocity, 9-11) and photomechanical single photon frequency shift. 12)

Graphene is a two-dimensional (2D) form of carbon, in which the atoms are placed in a honeycomb lattice. In the past few years, it has aroused wide public concern owing to its outstanding photonic and photoelectricity performances, ^{13,14} like broadband operation, high-speed operation and strong light graphene interaction. ¹⁵⁾ The carrier mobility is over 200 000 cm² V⁻¹ s⁻¹ at room temperature, and the absorption of monolayer graphene is as low as 2.3% in the infrared and visible range. ^{15–17)} In 2008, Wang et al. found the strong interband optical transitions of the graphene monolayer or bilayer, which can be significantly changed by electrical gating. ¹⁸⁾ This adjustability via adopting external voltage has been widely utilized for contriving optical devices in the past years. ^{15,19–27)}

In this letter, we investigate the high light confinement, field enhancement, and gradient force between two graphene layers, which may provide higher tunability than other 2D-materials. Furthermore, we clearly compare the different enhancement and light confinement at different wavelengths by showing the electric field distribution. On this basis, we analyze the gradient force of different intensity. In our simulation, a longer propagation length gives rise to higher Fermi energy, larger wavelength or wider separation. Higher Fermi energy, larger wavelength, or narrower separation should be applied to obtain a higher field enhancement. A larger confinement ratio can be achieved with higher Fermi energy, larger wavelength, or narrower separation. To sum

up, larger gradient force comes with lower Fermi energy, larger wavelength or narrower separation. These excellent performances may be conducive to optical manipulation at nanoscale and growth of photonic devices based on 2D materials.

As a distinctive feature of graphene, the complex conductivity can be effectively adjusted via changing the Fermi energy E_F (through the adopted electric field), chemical doping or ground plane evenness. Under such circumstances, graphene can exhibit properties of metals or dielectrics. Moreover, it can support both transverse magnetic (TM) and TE waveguide modes. The conductivity of graphene can be expressed as

$$\sigma_{g} = i \frac{e^{2} k_{B} T}{\pi \hbar^{2} (\omega + i \tau^{-1})} \left\{ \frac{E_{F}}{k_{B} T} + 2 \ln \left[\exp \left(-\frac{E_{F}}{k_{B} T} \right) + 1 \right] \right\} + i \frac{e^{2}}{4\pi \hbar^{2}} \ln \left[\frac{2|E_{F}| - \hbar(\omega + i \tau^{-1})}{2|E_{F}| + \hbar(\omega + i \tau^{-1})} \right].$$
(1)

In this expression, e denotes the electron charge, \hbar is the reduced Planck's constant, and k_B stands for the Boltzmann's constant. The first two terms of this formula are respectively introduced from the intraband and interband transition. At the room temperature, Fermi energy is invariably higher than half of photon energy for highly doped graphene in the simulated mid-infrared spectrum. Under such circumstances, thus, the intraband transition is in a dominant position and the interband transition is disregarded. The Kubo equation can be simplified to

$$\sigma_g = \frac{ie^2 E_F}{\pi \hbar^2 (\omega + i\tau^{-1})},\tag{2}$$

in which the carrier relaxation time is $\tau = \mu \mu_c / e v_f$, $\mu = 10\,000\,\mathrm{cm}^2~\mathrm{V}^{-1}~\mathrm{s}^{-1}$ is the carrier mobility and $v_f = c/300$ is the Fermi volicity in graphene. The graphene layer can be treated as an ultrathin slice. The permittivity can be expressed as

$$\varepsilon_g = \varepsilon_r + \frac{\sigma_g}{\omega \varepsilon_0 t_0}. (3)$$

In this equation, $t_0 = 0.34$ nm is the thickness of monolayer graphene. The surface plasmon polaritons modes can propagate in the monolayer graphene in the range from THz to the visible frequencies.

¹School of Science, Jiangnan University, Wuxi 214122, People's Republic of China

²School of Mechanical Engineering and Birck Nanotechnology Center, Purdue University, West Lafayette, Indiana 47907, United States of America

^{*}E-mail: jcwang@jiangnan.edu.cn

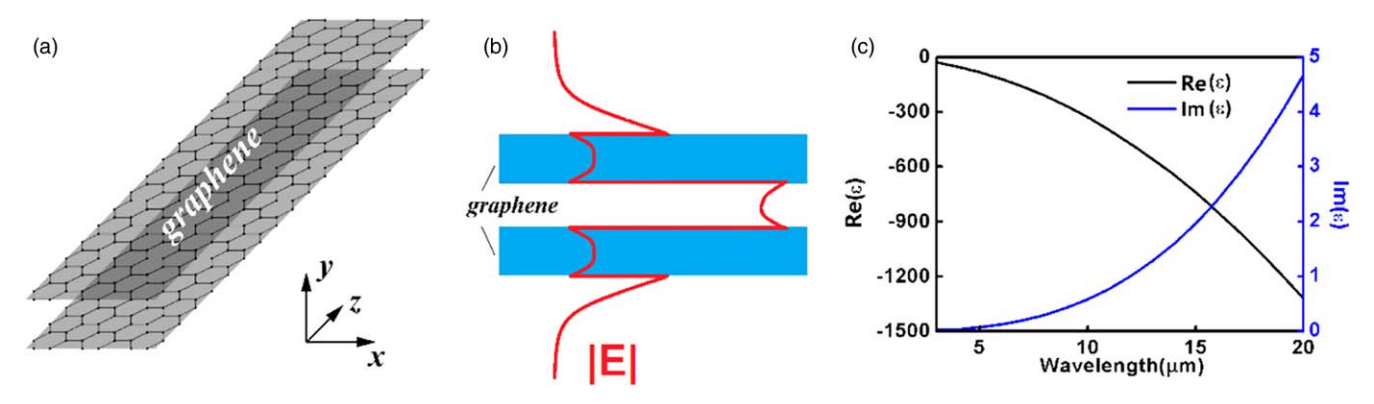


Fig. 1. (Color online) (a) The structure of the proposed face-to-face graphene layers; (b) diagrammatic sketch of the sectional view of the proposed structure and distribution of |E| along the y direction; (c) the relative permittivities of graphene when the Fermi energy $E_F = 0.3$ eV in the mid-infrared regions.

The schematic of graphene slot waveguide is exhibited in Figs. 1(a), 1(b) shows the sectional view of the structure. The two monolayer graphene waveguides with the same thickness t_0 are vertically aligned with a separation g. The length of the structure is $2 \mu m$ and the width can be seen as infinite. The fundamental mode propagates along the x direction.

In order to inspire the understanding of physics, the performance of a graphene slot waveguide is analyzed by adopting an analytical model of coupled ribbon waveguides. The field of the TM waves can be expressed by the following equations³¹⁾

$$\tan\left(-\frac{k_y t_0}{2} + \theta\right) = -\tan\left(\frac{k_y t_0}{2} + \theta\right) \tanh(\chi g). \tag{7}$$

Thus, based on above equations, the dispersion and field distributions of plasmonic modes can be educed.

Through integrating the Maxwell Stress Tensor around a discretional surface containing the graphene pairs, and the gradient force f_n can be calculated.³²⁾ By defining³³⁾

$$T_{ij} = \varepsilon_0 (E_i E_j - \delta_{ij} E^2 / 2) + \mu_0 (H_i H_j - \delta_{ij} H^2 / 2), \tag{8}$$

$$E_{y} = E_{0} \begin{cases} \cos\left(-\frac{k_{y}t_{0}}{2} + \theta\right) \cosh\left(\chi y\right) / \cosh\left(\chi \frac{g}{2}\right) & 0 < |y| < \frac{g}{2} \\ \frac{1}{\varepsilon_{y}} \cos\left[k_{y}\left(|y| - \frac{g}{2} - \frac{t_{0}}{2}\right) + \theta\right] & \frac{g}{2} < |y| < \frac{g}{2} + t_{0}, \\ \cos\left(\frac{k_{y}t_{0}}{2} + \theta\right) \exp\left[-\chi\left(|y| - \frac{g}{2} - t_{0}\right)\right] |y| > \frac{g}{2} + t_{0} \end{cases}$$

$$(4)$$

$$E_{x} = E_{0} \begin{cases} \frac{i\chi}{\beta} \cos\left(-\frac{k_{y}t_{0}}{2} + \theta\right) \sinh\left(\chi y\right) / \cosh\left(\chi \frac{g}{2}\right) & 0 < |y| < \frac{g}{2} \\ \frac{ik_{y}}{\beta \varepsilon_{x}} \sin\left[k_{y}\left(|y| - \frac{g}{2} - \frac{t_{0}}{2}\right) + \theta\right] & \frac{g}{2} < |y| < \frac{g}{2} + t_{0}, \\ \frac{i\chi}{\beta} \cos\left(\frac{k_{y}t_{0}}{2} + \theta\right) \exp\left[-\chi\left(|y| - \frac{g}{2} - t_{0}\right)\right] |y| > \frac{g}{2} + t_{0} \end{cases}$$

$$(5)$$

where θ stands for the phase shift of the optical field at the middle of each waveguide. The transverse vector in graphene ribbons k_y , the decay rate in air χ , and the propagation constant of the fundamental mode β are interrelated as follows:

$$\frac{\beta^2}{\varepsilon_y} + \frac{k_y^2}{\varepsilon_x} = k_0^2, \quad \beta^2 - \chi^2 = k_0^2, \tag{6}$$

where ε_y and ε_x are the anisotropic permittivity of graphene and k_0 is the vacuum wavenumber. By assuming that the tangential electric and magnetic field components are continuous at interface between graphene and air, the propagation constant β can be obtained by solving the equation below:

where δ is the Kronecker delta function, the normalized gradient force along the y direction is defined as

$$f_n = \oint_{S} TdS \cdot n_y, \tag{9}$$

where S is the surface of the volume containing the graphene pairs and n_y is the unit vector along the y direction. In conformity to the energy conservation law in the parallel graphene layers, this force can also be described as

$$f_n = \frac{1}{c} \frac{\partial n_{\text{eff}}}{\partial g} \bigg|_{\omega}.$$
 (10)

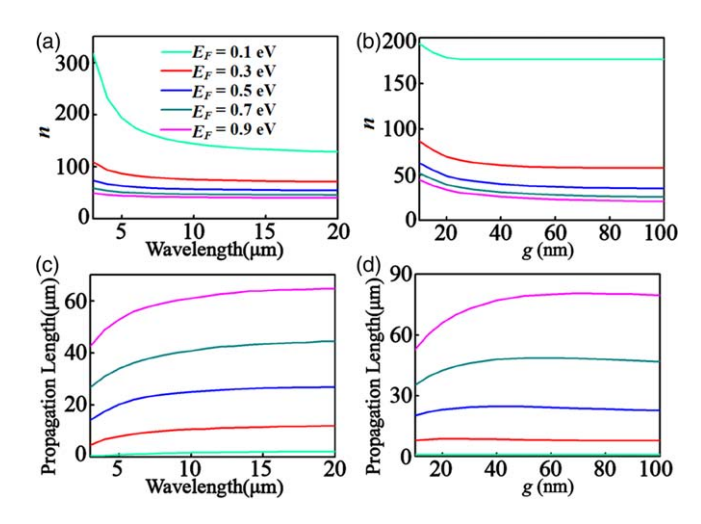


Fig. 2. (Color online) Dependence of the real effective index on the (a) wavelength and (b) gap distance and dependence of the propagation length on the (c) wavelength and (d) gap distance.

The dependence of the real effective refractive index and propagation length of the fundamental mode on the wavelength and the gap distance is shown in the Fig. 2. The Fermi energies are $E_F=0.1,\,0.3,\,0.5,\,0.7$ and 0.9 eV, respectively. The separation between the graphene pair is 10 nm in Figs. 2(a)–2(c) and the wavelength is 5 μ m in Figs. 2(b)–2(d). All simulations are performed using finite element method employing COMSOL Multiphysics.

In Fig. 2, the higher index can be achieved at a smaller wavelength, gap distance or lower Fermi energy, and a longer propagation length accompanied by a smaller effective refractive index. We can explain the dependencies in Fig. 2 by Eq. (6), $\beta^2/\varepsilon_y - k_y^2/|\varepsilon_x| = k_0^2$. As the wavelength decreases, the term k_0 increases, while $|\varepsilon_x|$ decreases. Because k_y solely rests with the geometric size of the waveguide along the y direction, the larger index and shorter propagation length can be obtained due to the smaller wavelength. Respecting the dependencies on the gap distance, the larger distance results in the smaller k_y , which further brings about a smaller index and longer propagation length. As we can see from Fig. 2, the propagation length can reach 63 μ m, and an even longer propagation length can be obtained by further increasing the Fermi energy.

The field enhancement is defined by the ratio of the electric field component $|E_y|$ in the slot region at y = g/2 to the one at upper graphene-air interface $y = g/2 + t_0$. The enhancement ratio can be educed from Eqs. (4) and (5):

ratio =
$$\sqrt{\frac{\chi^2 \varepsilon_x^2 + k_y^2}{\chi^2 \varepsilon_x^2 \tanh^2 (\chi g/2) + k_y^2}}.$$
 (11)

In addition, we analyzed the light confinement ratio, which is defined as the ratio of the integrated Poynting vector P_z in the domains between and outside the graphene layers

$$\xi = \int_{-d/2}^{d/2} P_z ds / \int_{-\infty}^{\infty} P_z ds. \tag{12}$$

As can be seen from Figs. 3 and 4, the enhancement is decreasing when the wavelength and Fermi energy decrease, or the gap distance increases. Similarly, just as Fig. 3(c) shows, the field components of $|E_y|$ and E_z are more strongly confined in the two graphene layers as the wavelength

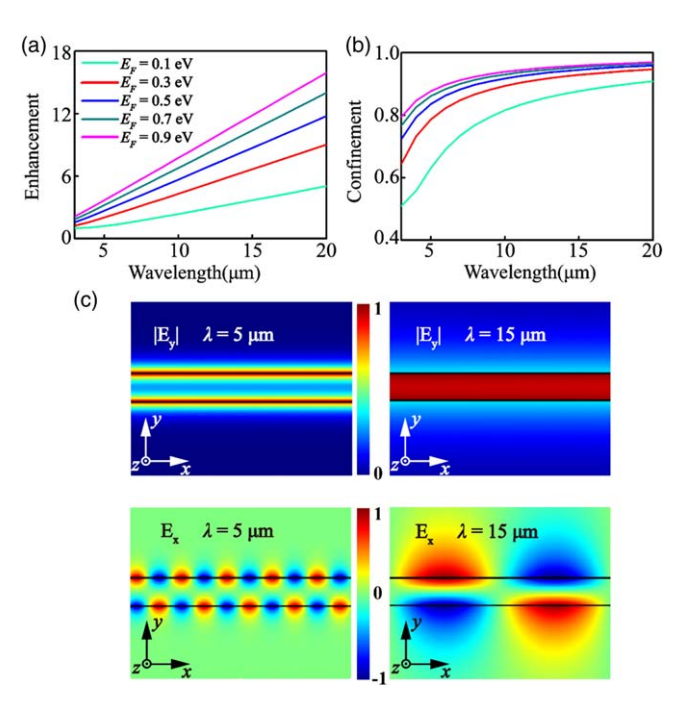


Fig. 3. (Color online) Dependence of the (a) enhancement and (b) confinement ratios on the wavelength. (c) Field profiles of $|E_y|$ and E_z with different wavelength, respectively. The separation of the graphene pair is 10 nm.

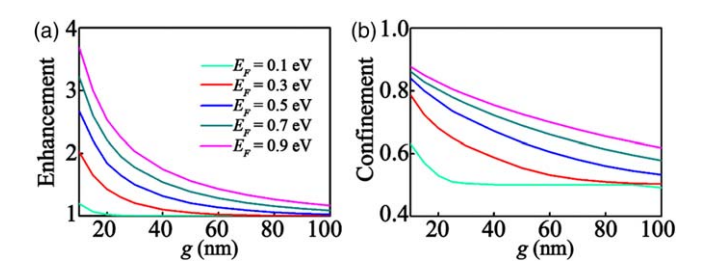


Fig. 4. (Color online) Dependence of the (a) enhancement and (b) confinement ratios on the gap distance. The wavelength is 5 μ m.

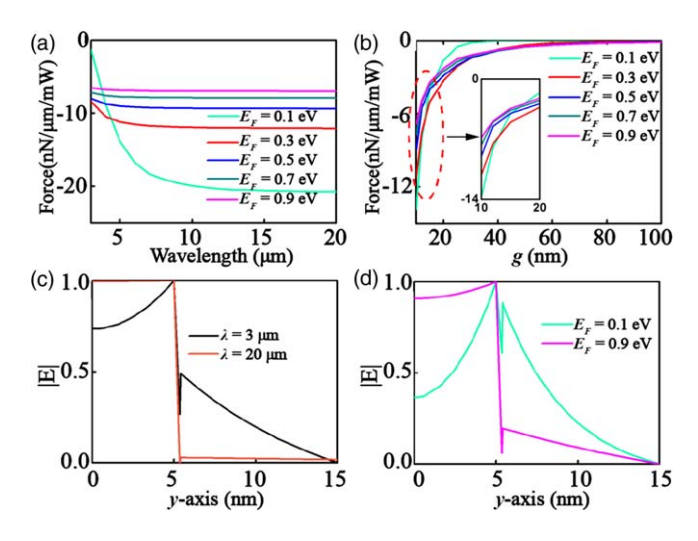


Fig. 5. (Color online) The optical gradient force with different (a) wavelength and (b) gap distance. Distributions of |E| along the *y*-axis with different (c) wavelength and (d) Fermi energy.

decreases, which weakens the enhancement. In the meantime, as the separation d decreases, the interactions between the graphene layers get stronger. As a result, a larger field enhancement is obtained. Mathematically, on the basis of

Fig. 2(a) and Eq. (6), the decreasing wavelength or Fermi energy results in the larger propagation constant β and decay rate χ . The value of $\tanh 2(\chi g/2)$ in Eq. (11) increases as χ increases while it is located within [0, 1], which causes a smaller enhancement.

In Figs. 3(b) and 4(b), the light confinement ratio can be enhanced via higher Fermi energy while it decreases as the wavelength decreases. The higher symmetry of the field profile gives rise to the increasing power propagating within $y = [g/2 + d, \infty]$. Owing to this, the lower confinement ratio is obtained. As can be seen from Fig. 4(b), the ratio diminishes as the separation increases. When the separation of the graphene pair is 10 nm and the wavelength is 20 μ m, the enhancement can reach 18 and the light confinement ratio is nearly 97%. Furthermore, they can be even higher with a longer wavelength or Fermi energy.

The dependence of gradient force on the wavelength and separation is severally shown in Figs. 5(a) and 5(b). The separation of the graphene pair in Fig. 5(a) is 10 nm, and the wavelength in Fig. 5(b) is 5 μ m. To deepen the understanding of the mechanism behind, we show the distribution of a normalized electric field |E| along the y-axis in Figs. 5(c) and 5(d). Just as Fig. 5(a) shows, a negative value implies an attractive force. It can be enhanced with a smaller Fermi energy or longer wavelength. While the wavelength is less than $6 \mu m$, it suddenly diminishes since the wavelength decreases owing to the weaker interaction between the graphene pair. When the wavelength is longer than 4.5 μ m, the optical gradient force is stronger with a lower Fermi energy. Figure 5(b) shows that the lower Fermi energy or narrower separation of the graphene pair is when the gap distance g is shorter than 13 nm, the stronger optical gradient force will be acquired. However, while the gap distance is longer than 40 nm, the optical gradient force decreases with a longer gap distance or a lower Fermi energy. In addition, it can be further enhanced by enlarging the wavelength, diminishing the separation of the graphene pair or reducing the Fermi energy. By contrasting Figs. 4(a) and 5(b), we can find that the largest enhancement is accompanied by the weakest force when the separation between the graphene pair is 10 nm. It can be explicated by the distribution of |E|. Although the enhancement ratio at 0.1 eV is lower than that at 0.9 eV, the slope of |E| in the region $y = [g/2 + d, \infty]$ is much larger when $E_F = 0.1 \text{ eV}$. On account of the strong dependence of gradient force on the gradient of field damping, this force should be much stronger at 0.1 eV than that at 0.9 eV.

To summarize, we have proposed a new method to acquire high light confinement, field enhancement, and gradient force via uniting a slot waveguide structure with graphene. Higher Fermi energy, longer wavelength or wider separation give rise to a longer propagation length. If higher field enhancement is needed, higher Fermi energy, longer wavelength, or narrower separation should be applied. Higher Fermi energy, longer wavelength, or narrower separation contributes to a higher confinement ratio. Overall, stronger gradient force can be acquired with lower Fermi energy, larger wavelength or narrower separation. With the gap distance g = 100 nm, the wavelength $\lambda = 5 \, \mu \text{m}$ and the Fermi energy $E_F = 0.9 \, \text{eV}$, a

propagation length as long as 79.5 μ m can be achieved. With the wavelength $\lambda = 20~\mu$ m, the gap distance $g = 10~\rm nm$ and the Fermi energy $E_F = 0.9~\rm eV$, an enhancement ratio up to 16 and a light confinement ratio up to 97% can be obtained. An optical gradient force $f = 20~\rm nN~\mu m^{-1}~mW^{-1}$ can be achieved with $E_F = 0.9~\rm eV$ and the gap distance $g = 10~\rm nm$. And the results can be even better by tuning the wavelength, the gap distance and the Fermi energy. These superior performances would contribute to optical manipulations at the nanoscale level as well as the growth of graphene-based photonic devices.

Acknowledgments This work is supported by the National Natural Science Foundation of China (Grant No. 11504139, 11504140, 11811530052), the China Postdoctoral Science Foundation (2017M611693, 2018T110440), and the National Science Foundation (CMMI-1405078, CMMI-1554189, CMMI-1634832).

ORCID iDs Zheng-Da Hu https://orcid.org/0000-0001-5655-3331

- A. Ashkin and J. M. Dziedzic, "Optical levitation in high vacuum," Appl. Phys. Lett. 28, 333 (1976).
- X. Sun, J. Zheng, M. Poot, C. W. Wong, and H. X. Tang, "Femtogram doubly clamped nanomechanical resonators embedded in a high-q twodimensional photonic crystal nanocavity," Nano Lett. 12, 2299 (2012).
- H. Li, J. W. Noh, Y. Chen, and M. Li, "Enhanced optical forces in integrated hybrid plasmonic waveguides," Opt. Express 21, 11839 (2013).
- Z. Huang, K. Cui, G. Bai, X. Feng, F. Liu, W. Zhang, and Y. Huang, "High-mechanical-frequency characteristics of optomechanical crystal cavity with coupling waveguide," Sci. Rep. 6, 34160 (2016).
- X. Xu, L. Shi, Y. Liu, Z. Wang, and X. Zhang, "Enhanced optical gradient forces between coupled graphene sheets," Sci. Rep. 6, 28568 (2016).
- 6) M. L. Povinelli, M. Lončar, M. Ibanescu, E. J. Smythe, S. G. Johnson, F. Capasso, and J. D. Joannopoulos, "Evanescent-wave bonding between optical waveguides," Opt. Lett. 30, 3042 (2005).
- Y. W. Hu, Y. F. Xiao, Y. C. Liu, and Q. Gong, "Optomechanical sensing with on-chip microcavities," Front. Phys. 8, 475 (2013).
- M. Bagheri, M. Poot, L. Fan, F. Marquardt, and H. X. Tang, "Photonic cavity synchronization of nanomechanical oscillators," Phys. Rev. Lett. 111, 213902 (2013).
- Z. Wang, L. Shi, Y. Liu, X. Xu, and X. Zhang, "Optical nonreciprocity in asymmetric optomechanical couplers," Sci. Rep. 5, 8657 (2015).
- 10) K. Fang, J. Luo, A. Metelmann, M. H. Matheny, F. Marquardt, A. A. Clerk, and O. Painter, "Generalized nonreciprocity in an optomechanical circuit via synthetic magnetism and reservoir engineering," Nat. Phys. 13, 465 (2017).
- 11) E. Verhagen and A. Alù, "Optomechanical nonreciprocity," Nat. Phys. 13, 922 (2017).
- 12) L. Fan, C. L. Zou, M. Poot, R. Cheng, X. Guo, X. Han, and H. X. Tang, "Integrated optomechanical singlephoton frequency shifter," Nat. Photonics 10, 766 (2016).
- 13) F. H. L. Koppens, D. E. Chang, and F. J. G. De Abajo, "Graphene plasmonics: a platform for strong light," Nano Lett. 11, 3370 (2011).
- 14) F. Bonaccorso, Z. Sun, T. Hasan, and A. C. Ferrari, "Graphene photonics and optoelectronics," Nat. Photonics 4, 611 (2010).
- 15) M. Liu, X. Yin, E. Ulin-Avila, B. Geng, T. Zentgraf, L. Ju, F. Wang, and X. Zhang, "A graphene-based broadband optical modulator," Nature 474, 64 (2011)
- 16) R. R. Nair, P. Blake, A. N. Grigorenko, K. S. Novoselov, T. J. Booth, T. Stauber, N. M. R. M. R. Peres, and A. K. Geim, "Fine structure constant defines visual transparency of graphene," Science 320, 1308 (2008).
- 17) K. I. Bolotin, K. J. Sikes, Z. Jiang, M. Klima, G. Fudenberg, J. Hone, P. Kim, and H. L. Stormer, "Ultrahigh electron mobility in suspended graphene," Solid State Commun. 146, 351 (2008).
- 18) F. Wang, Y. Zhang, C. Tian, C. Girit, A. Zettl, M. Crommie, and Y. R. Shen, "Gate variable optical transitions in graphene," Science 320, 206 (2008).
- 19) T. Mueller, F. Xia, and P. Avouris, "Graphene photodetectors for high-speed optical communications," Nat. Photonics 4, 297 (2010).
- V. Sorianello, M. Midrio, and M. Romagnoli, "Design optimization of single and double layer graphene phase modulators in SOI," Opt. Express 23, 6478 (2015).
- 21) M. Liu, X. Yin, and X. Zhang, "Double-layer graphene optical modulator," Nano Lett. 12, 1482 (2012).

- 22) W. Gao, J. Shu, C. Qiu, and Q. Xu, "Excitation of plasmonic waves in graphene by guided-mode resonances," ACS Nano 6, 7806 (2012).
- 23) M. Fan, H. Yang, P. Zheng, G. Hu, B. Yun, and Y. Cui, "Multilayer graphene electro-absorption optical modulator based on double-stripe silicon nitride waveguide," Opt. Express 25, 21619 (2017).
- 24) H. Qian et al., "Electrical tuning of surface plasmon polariton propagation in graphene-nanowire hybrid structure," ACS Nano 8, 2584 (2014).
- 25) L. Vicarelli, M. S. Vitiello, D. Coquillat, A. Lombardo, A. C. Ferrari, W. Knap, M. Polini, V. Pellegrini, and A. Tredicucci, "Graphene field-effect transistors as roomtemperature terahertz detectors," Nat. Mater. 11, 865 (2012).
- 26) S. J. Koester and M. Li, "High-speed waveguide-coupled grapheneon-graphene optical modulators," Appl. Phys. Lett. 100, 171107 (2012).
- J. S. Shin and J. T. Kim, "Broadband silicon optical modulator using a graphene-integrated hybrid plasmonic waveguide," Nanotechnology 26, 365201 (2015).

- 28) B. Zhu, G. Ren, Y. Gao, H. Li, B. Wu, and S. Jian, "Strong light confinement and gradient force in a hexagonal boron nitride slot waveguide," Opt. Lett. 41, 4991 (2016).
- 29) D. Mao, H. Lu, J. Zhao, X. Gan, and Y. Gong, "Strong plasmonic confinement and optical force in phosphorene pairs," Opt. Express 25, 5255 (2017).
- 30) K. S. Novoselov, A. K. Geim, S. V. Morozov, D. Jiang, Y. Zhang, S. V. Dubonos, I. V. Grigorieva, and A. A. Firsov, "Electric field effect in atomically thin carbon films," Science 306, 666 (2004).
- 31) V. R. Almeida, Q. Xu, C. A. Barrios, and M. Lipson, "Guiding and confining light in void nanostructure," Opt. Lett. 29, 1209 (2004).
- J. D. Jackson, Classical Electrodynamics (Wiley, New York, 1998) 3rd ed., p. 258.
- 33) L. Novotny and B. Hecht, *Principles of Nano-Optics* (Cambridge University Press, Cambridge, 2006).